

Phase transition temperatures and electrical properties of divalent ions (Ca^{2+} , Sr^{2+} and Ba^{2+}) substituted $(\text{Bi}_{1/2}\text{Na}_{1/2})\text{TiO}_3$ ceramics

Y. Watanabe, Y. Hiruma, H. Nagata, T. Takenaka*

Faculty of Science and Technology, Tokyo University of Science, Yamazaki 2641, Noda, Chiba 278-8510, Japan

Available online 4 October 2007

Abstract

Phase transition temperature and electrical properties of divalent ions (Ca^{2+} , Sr^{2+} and Ba^{2+}) substituted $(\text{Bi}_{1/2}\text{Na}_{1/2})\text{TiO}_3$ (BNT)-based ceramics were studied to investigate the relationship between the substituted ion and the effect on various characteristics. These ceramics were prepared by a conventional ceramic fabrication process. The behavior of the depolarization temperature, T_d , slope depends on the substituted ionic radius before correspondence of the T_d to the rhombohedral–tetragonal phase transition temperature, T_{R-T} (0–3 at% for Ba^{2+} -substituted BNT). The piezoelectric constant, d_{33} , of Ca^{2+} and Sr^{2+} increased because of the increase of their free permittivity, $\epsilon_{33}^T/\epsilon_0$, accompanying a decrease of T_d . On the other hand, the d_{33} of Ba^{2+} -substituted BNT increased with increasing amount of Ba^{2+} below 7 at% because Ba^{2+} -substituted BNT has a MPB composition. Therefore, the d_{33} of Ba^{2+} 7 at% substituted BNT had a maximum of 152 pC/N. T_d has a trade-off relationship with d_{33} .
© 2007 Elsevier Ltd and Techna Group S.r.l. All rights reserved.

Keywords: C. Piezoelectric properties; C. Dielectric properties; D. Perovskite

1. Introduction

Recently, there has been greater concern about environmental protection for the piezoceramics, because of the concern regarding the detrimental effect of lead on the environment and the human body, the research and development of a high-performance lead-free piezoelectric material is urgently required. It is necessary that the operating temperature is more than 200 °C and the dielectric constant, d_{33} , is more than 300 pC/N for actuators. Bismuth sodium titanate $(\text{Bi}_{1/2}\text{Na}_{1/2})\text{TiO}_3$ (BNT) has attracted attention as one of the candidates for a lead-free actuator material. For BNT, it has been reported that excess-Bi BNT (BNT + Bi_2O_3 0.3 wt%) has a piezoelectric constant of $d_{33} = 93.4$ pC/N, and for La 2.0 at% substituted BNT, $d_{33} = 91$ pC/N [1,2]. BNT ceramics with compositions around the morphotropic phase boundary (MPB) were investigated [3,4]. Also, it was reported that phase transition temperatures such as the second-phase transition temperature of the rhombohedral–tetragonal phase transition, T_{R-T} , and the Curie temperature of the tetragonal–cubic phase transition, T_{T-C} , are about 300 and 540 °C, respectively [5,6]. Moreover,

divalent-ion substituted BNT solid solutions have also been investigated [7–11]. On the other hand, the BNT ceramic has the disadvantage of its narrow operating temperature range, because of its depolarization temperature, T_d , of 183 °C at which piezoelectricity disappears. However, there are few reports on this disadvantage, even though this characteristic is very important for practical use.

In this study, we investigated the electrical properties and phase transition temperatures such as the depolarization temperature, T_d , the rhombohedral–tetragonal phase transition temperature, T_{R-T} , and the maximum permittivity temperature, T_m , of BNT and divalent-ion (Ca^{2+} , Sr^{2+} and Ba^{2+})-substituted BNT ceramics. The evaluation of T_d , T_{R-T} and T_m was carried out by determining the temperature dependence of the dielectric and piezoelectric properties [12]. These divalent elements were chosen to find out the effect of the substituted ionic radius; the ionic radii of six coordinates for Ca^{2+} , Sr^{2+} and Ba^{2+} are 1.00, 1.18 and 1.35 Å, respectively, from the work of Shannon [13].

2. Experimental procedure

In this paper, the compositions of the prepared samples with the formula $(\text{Bi}_{1/2}\text{Na}_{1/2})_{1-x}\text{A}_x\text{TiO}_3$ [$\text{A} = \text{Ca}^{2+}$, Sr^{2+} and Ba^{2+}] are denoted by BNCT100x, BNST100x and BNBT100x, respectively. The values of x in the prepared compositions of

* Corresponding author. Tel.: +81 4 7122 9539; fax: +81 4 7123 0856.

E-mail address: tadashi@ee.noda.tus.ac.jp (T. Takenaka).

divalent-ion (Ca^{2+} , Sr^{2+} and Ba^{2+})-substituted BNT are 0–0.08, 0.28 and 0.20, respectively. These ceramics were prepared by a conventional ceramic fabrication process. The starting materials were Bi_2O_3 , Na_2CO_3 , TiO_2 , CaCO_3 , SrCO_3 and BaCO_3 with purities of 3–4N. They were weighed at a stoichiometry ratio and milled with zirconia balls in ethanol for 10 h. The mixed powders were calcined at 800 °C for 2 h in a zirconia crucible and ball-milled again for 20 h after grinding. After pressing by cold isostatic pressing (CIP) at 150 MPa, the powders were sintered at 1100–1150 °C for 2 h in air. Sintered samples were cut to a predetermined measurement shape and fired-on silver paste was used as the electrodes for electrical measurements.

X-ray powder diffraction measurements of sintered samples were performed using X-ray diffractometer (Rigaku, RINT2000) using Cu K α radiation. In the electrical measurements, dielectric and piezoelectric properties were measured. Dielectric properties were measured for samples both before and after poling by means of a multi frequency LCR meter (Wayne Kerr 6440B). To determine piezoelectric properties, samples were poled with a dc field of 5–6 kV/mm for 4–7 min in a silicone oil bath at R.T. and were measured using an impedance analyzer (HP 4294A). The longitudinal vibration in the (33)-mode was measured using a solid rectangular specimen of 2 mm \times 2 mm \times 5 mm, then the piezoelectric constant, d_{33} , was calculated using a resonance and anti resonance method. Also, the value of dynamic d_{33} was measured by means of a strain meter (Millitron 1240).

3. Results and discussion

All samples studied here were solid solutions with a perovskite structure, as shown by X-ray powder diffraction measurements at R.T. The relative densities of all the samples were higher than 95% of the theoretical densities. The resistivity of all samples were higher than $1 \times 10^{12} \Omega\cdot\text{cm}$. Fig. 1 shows the lattice constants, a and c , and rhombohedral distortion, $90^\circ - \alpha$, as a function of x for BNCT100 x and BNST100 x . It is shown that the lattice distortion of both specimens decreases with increasing x , although lattice constants have different tendencies. It is thought that the lattice constant decreased after Ca^{2+} substitution because its ionic radius is smaller than the average A-site ionic radius of BNT. Also, the lattice constant increased after Sr^{2+} substitution for the opposite reason.

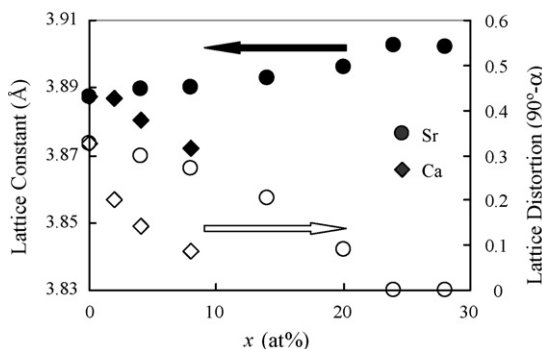


Fig. 1. Dependences of lattice constant and lattice distortion as a function of x in BNCT100 x and BNST100 x .

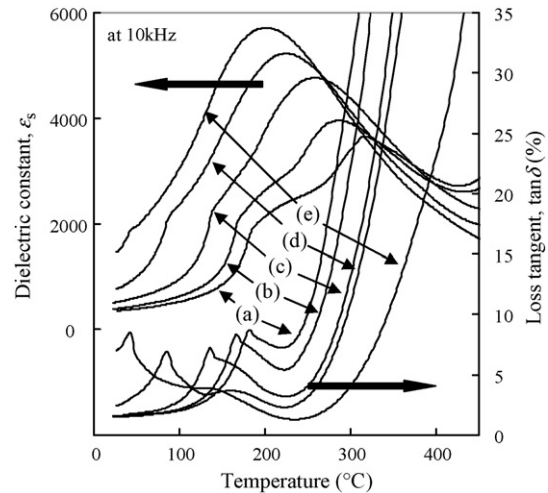


Fig. 2. Temperature dependences of poled dielectric constant, ϵ_s , and $\tan \delta$ for BNST100 x : (a) $x = 0.04$, (b) $x = 0.08$, (c) $x = 0.14$, (d) $x = 0.20$ and (e) $x = 0.24$.

The temperature dependence of the dielectric constant of BNST100 x at 10 kHz after poling is shown in Fig. 2. The peak loss tangent, $\tan \delta$, gives T_d at that composition. T_d and T_m shift to lower temperature with increasing x . T_d for BNST24 was 42 °C. Also, the maximum permittivity increased with increasing x . It is found that after poling at R.T., ϵ_s increased with increasing x . This figure indicates that increasing permittivity is accompanied by a decrease in T_d , which eventually decreases below R.T. Slightly different behavior could be observed for the other kinds of compositions. In the case of Ca^{2+} substitution, T_m shifts to a higher temperature with increasing x . For Ba^{2+} substitution, the behaviors of phase transition temperatures did not show a monotonic tendency because of morphotropic phase boundary (MPB) composition.

Fig. 3 shows T_d , T_{R-T} and T_m for (a) BNCT100 x , (b) BNST100 x and (c) BNBT100 x . Phase diagrams of these prepared samples obtained by dielectric measurement are indicated in this figure. For Ca^{2+} substitution, T_d and T_{R-T} decreased and T_m increased with increasing x . However, T_m for Sr^{2+} and Ba^{2+} substitution decreased with increasing x . T_d and T_{R-T} for Sr^{2+} substitution decreased with increasing x , as shown in Fig. 2. Decrease of rhombohedral distortion seems to relate to T_d as shown in Fig. 1. In terms of T_d , the piezoelectricity of BNCT100 x will disappear at about $x = 0.11$ and that of BNST100 x disappears at about $x = 0.26$ from the extension of the T_d curves. Ba^{2+} substitution results in a different phase diagram compared with the two other systems. T_d increased up to $x = 0.04$, at which T_d corresponds to T_{R-T} . Because the slopes of T_d and T_{R-T} are dominated by the T_{R-T} transition, both temperatures decreased with increasing x for higher values of x , as for Ca^{2+} and Sr^{2+} substitution. However, at $x = 0.07$, T_{R-T} decreased intact and T_d increased. The T_d slopes are closely related to the substituted ionic radius in the study of lanthanoid-substituted BNT [14]. In the case of divalent-ion substitution, the T_d slopes of the specimens depend on the substituted ionic radius until $x = 0.04$.

The dependence of $\epsilon_{33}^T/\epsilon_0$ and k_{33} on x in BNCT100 x , BNST100 x and BNBT100 x are shown in Figs. 4 and 5,

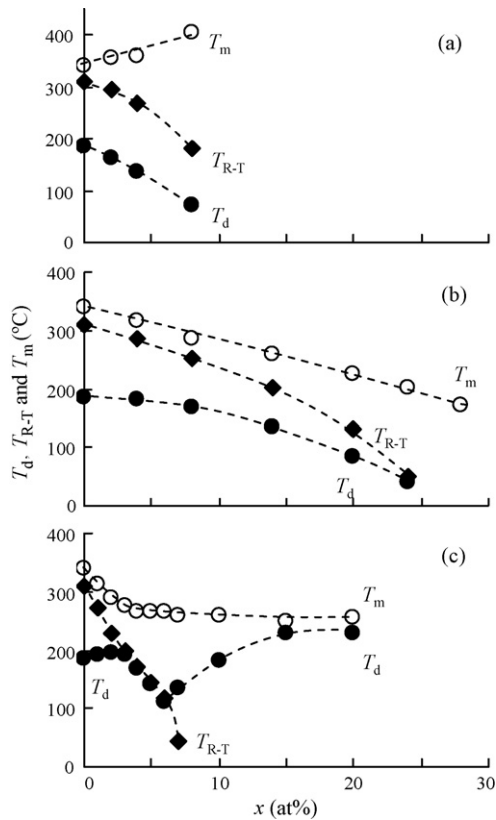


Fig. 3. Phase transition temperatures, T_d , T_{R-T} and T_m , as a function of x in (a) BNCT100x, (b) BNST100x and (c) BNBT100x.

respectively. $\epsilon_{33}^T/\epsilon_0$ generally increased with increasing x . For Sr^{2+} substitution, the wave pattern of ϵ_s was shifted to lower temperatures with increasing x , as shown in Fig. 2; therefore, the increase of $\epsilon_{33}^T/\epsilon_0$ can be understood. The values of k_{33} for Ca^{2+} and Sr^{2+} substitution initially increase with x , and then decrease accompanying a decrease of T_d to R.T. For Ba^{2+} , both characteristics increase rapidly and showed high values at MPB composition. k_{33} decreased at BNBT10. k_{33} and $\epsilon_{33}^T/\epsilon_0$ had maximum values of 0.447 and 369 for BNCT2, 0.509 and 836 for BNST20, 0.535 and 865 for BNBT7, respectively.

The piezoelectric constants, d_{33} , calculated using the resonance and anti resonance method for BNCT100x, BNST100x and BNBT100x are shown in Fig. 6. Each value

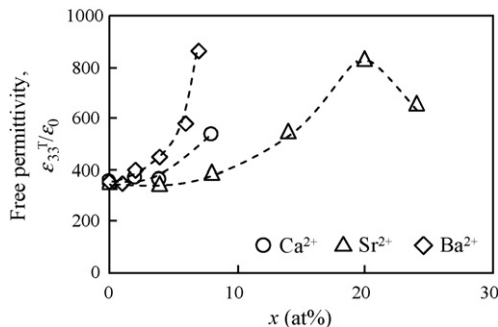


Fig. 4. Free permittivity, $\epsilon_{33}^T/\epsilon_0$, as a function of x in BNCT100x, BNST100x and BNBT100x.

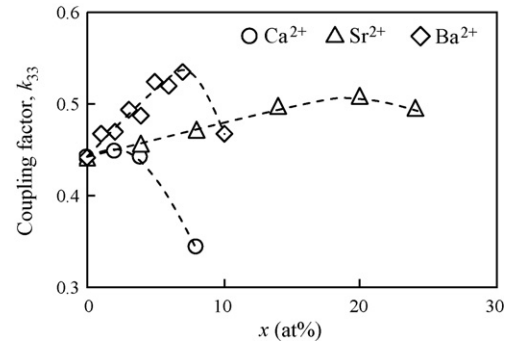


Fig. 5. Coupling factor, k_{33} , as a function of x in BNCT100x, BNST100x and BNBT100x.

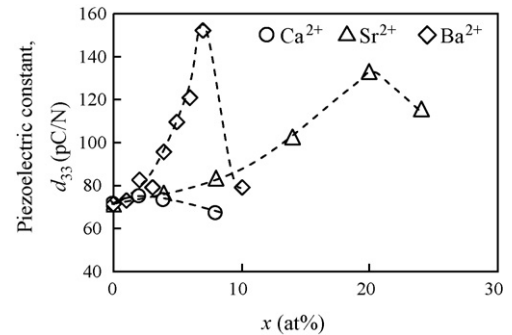


Fig. 6. Piezoelectric constants, d_{33} , as a function of x in BNCT100x, BNST100x and BNBT100x.

increased initially, then exhibited the maximum at $x = 0.02$ for Ca^{2+} , at $x = 0.20$ for Sr^{2+} and at $x = 0.07$ for Ba^{2+} . Before the maximum, the increase of the k_{33} and $\epsilon_{33}^T/\epsilon_0$ brings the enhancement of d_{33} . In contrary, after the maximum, d_{33} value decreased with proportional to the decrease of the k_{33} value. That is because the T_d was shifted closely to R.T. But in the case of Ba^{2+} substitution, there is one composition at which d_{33} showed a relative maximum because of the MPB composition at about $x = 0.06$ – 0.07 . Then, d_{33} decreased in the tetragonal phase. The d_{33} of BNT ceramics is 71 pC/N. On the other hand, the d_{33} of BNBT7 had a maximum of 152 pC/N. The maximum values of d_{33} for BNCT2 and BNST20 were 75 and 133 pC/N, respectively. These values are high compared with that for BNT.

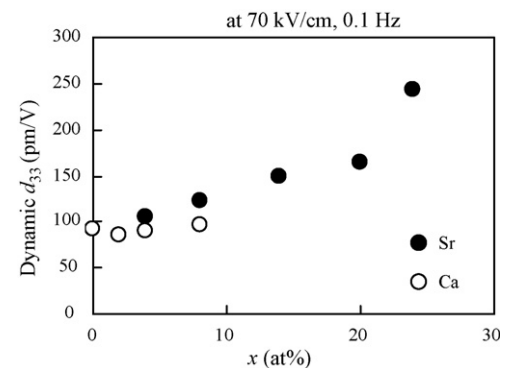


Fig. 7. Dynamic d_{33} as a function of x in BNCT100x and BNST100x at 70 kV/cm and 0.1 Hz.

Another d_{33} measurement was also carried out. The results of piezoelectric strain measurements for Ca^{2+} - and Sr^{2+} -substituted BNT are shown in Fig. 7 and exhibited similar tendencies to the results obtained by the resonance and antiresonance method. These values increase until slightly before disappearance of T_d because the permittivity increased, and are generally higher than the values obtained by the resonance and anti resonance methods. In particular, it is difficult to pole samples of BNCT8; thus, its d_{33} did not have a high value.

4. Conclusions

In this study, the phase transition temperatures and electrical properties of divalent-ion (Ca^{2+} , Sr^{2+} and Ba^{2+})-substituted BNT ceramics were investigated. The results are summarized as follows.

- (1) T_d was associated with a decrease of rhombohedral distortion, except for Ba^{2+} substitution.
- (2) The T_d slopes of the specimens depend on the substituted ionic radius until $x = 0.04$.
- (3) d_{33} tends to increase with decreasing T_d , because $\varepsilon_{33}^T/\varepsilon_0$ increased simultaneously.
- (4) The maximum values of d_{33} for BNCT2, BNST20 and BNBT7 were 75, 133 and 152 pC/N, respectively.
- (5) The dynamic d_{33} increased with d_{33} . These values were calculated using the resonance and anti resonance method. The measured values of dynamic d_{33} were higher than those calculated by resonance and anti resonance method.

References

- [1] H. Nagata, T. Shinya, Y. Hiruma, T. Takenaka, Piezoelectric properties of bismuth sodium titanate ceramics, *Ceram. Trans. Dev. Dielectr. Mater. Electron. Dev.* 167 (2004) 213–221.
- [2] A. Herabut, A. Safari, Processing and electromechanical properties of $(\text{Bi}_{1/2}\text{Na}_{1/2})_{(1-1.5x)}\text{La}_x\text{TiO}_3$ ceramics, *J. Am. Ceram. Soc.* 80 (1997) 2954–2958.
- [3] S. Zhang, T.R. Shrout, H. Nagata, Y. Hiruma, T. Takenaka, Piezoelectric properties in $(\text{K}_{0.5}\text{Bi}_{0.5})\text{TiO}_3$ – $(\text{Na}_{0.5}\text{Bi}_{0.5})\text{TiO}_3$ – BaTiO_3 lead-free ceramics, *IEEE Trans. Ultrason. Ferroelectr. Freq. Contr.* 54 (2007) 910–917.
- [4] H.D. Li, C.D. Feng, W.L. Yao, Some effects of different additives on dielectric and piezoelectric properties of $(\text{Bi}_{1/2}\text{Na}_{1/2})\text{TiO}_3$ – BaTiO_3 morphotropic phase boundary composition, *Mater. Lett.* 58 (2004) 1194–1198.
- [5] J.A. Zvirgzds, P.P. Kapostin, J.V. Zviagzde, T.V. Kruzina, X-ray study of phase transitions in ferroelectric $\text{Na}_{0.5}\text{Bi}_{0.5}\text{TiO}_3$, *Ferroelectrics* 40 (1982) 75–77.
- [6] I.P. Pronin, P.P. Syrnikov, V.A. Isupov, V.M. Egorov, N.V. Zaitseva, A.F. Ioffe, Peculiarities of phase transitions in sodium–bismuth titanate, *Ferroelectrics* 25 (1980) 395–397.
- [7] J. Suchanicz, M.G. Gavshin, A.Y. Kudzin, C. Kus, Dielectric properties of $(\text{Na}_{0.5}\text{Bi}_{0.5})_{1-x}\text{Me}_x\text{TiO}_3$ ceramics near morphotropic phase boundary, *J. Mater. Sci.* 36 (2001) 1981–1985.
- [8] S. Park, K.S. Hong, Phase relations in the system of $(\text{Na}_{1/2}\text{Bi}_{1/2})\text{TiO}_3$ – PbTiO_3 , I. Structure, *J. Appl. Phys.* 79 (1996) 383–387.
- [9] S. Park, K.S. Hong, Variations of structure and dielectric properties on substituting A-site cations for Sr^{2+} $(\text{Na}_{1/2}\text{Bi}_{1/2})\text{TiO}_3$, *J. Mater. Res.* 12 (1997) 2152–2157.
- [10] K. Sakata, Y. Masuda, Ferroelectric and antiferroelectric properties of $(\text{Na}_{0.5}\text{Bi}_{0.5})\text{TiO}_3$ – SrTiO_3 solid solution ceramics, *Ferroelectrics* 7 (1974) 347–349.
- [11] T. Takenaka, K. Maruyama, K. Sakata, $(\text{Bi}_{1/2}\text{Na}_{1/2})\text{TiO}_3$ – BaTiO_3 System for lead-free piezoelectric ceramics, *Jpn. J. Appl. Phys.* 30 (1991) 2236–2239.
- [12] Y. Hiruma, H. Nagata, T. Takenaka, Phase transition temperatures and piezoelectric properties of $(\text{Bi}_{1/2}\text{Na}_{1/2})\text{TiO}_3$ – $(\text{Bi}_{1/2}\text{K}_{1/2})\text{TiO}_3$ – BaTiO_3 lead-free piezoelectric ceramics, *Jpn. J. Appl. Phys.* 45 (2006) 7409–7412.
- [13] R.D. Shannon, Revised effective ionic radii and systematic studies of interatomic distances in halides and chalcogenides, *Acta Crystallogr. Sect. A* 32 (1976) 751–767.
- [14] Y. Hiruma, Y. Watanabe, H. Nagata, T. Takenaka, The behavior of phase transition temperatures for A-site substituted $(\text{Bi}_{1/2}\text{Na}_{1/2})\text{TiO}_3$ -based ferroelectric ceramics, *Key Eng. Mater.* 350 (2007) 93–96.